

# EXPERIMENTAL INVESTIGATION ON SHEAR STRENGTHENING OF CORRODED REINFORCED CONCRETE COLUMNS BY PET FIBERS WITH LARGE FRACTURING STRAIN

Dawei Zhang <sup>1,\*</sup>, Yuxi Zhao<sup>1</sup> and Tamon Ueda<sup>2</sup>

<sup>1</sup> Institute of Structural Engineering,

College of Architecture and Civil Engineering, Zhejiang University

866 Yuhangtang Road, Hangzhou, China 310058.\*Email: dwzhang@zju.edu.cn

<sup>2</sup> Lab of Engineering for Maintenance System, Hokkaido University,

Nishi 13 Chome, Kita 8 Jo, Sapporo, Japan 060-0808

## ABSTRACT

The seismic strengthening of the concrete columns improperly designed or constructed is in an urgent need. There has been an enormous interest in the research and application of conventional fiber reinforced polymers (FRPs) in RC column seismic retrofitting. However, due to low fracturing strain capacity of conventional FRPs, the fiber materials tend to fail sooner due to fiber breakage. New fiber materials such as polyacetal fiber (PAF), polyethylene naphthalate (PEN) and polyethylene terephthalate (PET) have properties of large fracturing strain and low stiffness in comparison to aramid, carbon, and glass fibers. In this paper, an experimental study is presented on the influence of PET warping on shear capacity, ductility and energy absorptivity of RC columns with stirrup corrosion before strengthening. The experimental program involved an electrochemical process to accelerate the migration of chlorides from an external electrolyte into the tested columns, a wetting – drying cycle process with a controlled current to speed up the corrosion of the stirrup in the tested columns, the strengthening of corroded columns with PET warping, and a Pseudo static test to determine the shear capacity of the tested beams. The shear performance of PET wrapped RC columns with different corrosion levels in stirrups, including the yield strength, the peak strength, the ductility ratio and the energy dissipation ability was examined and the related mechanism was discussed.

## KEYWORDS

Corrosion, strengthening, ductility, energy dissipation, column.

## INTRODUCTION

Even though many latest design specifications in the world specifies confinement regions at the ends of columns and beams to ensure their seismic resistance, field observations indicated that this requirement was not followed in many buildings, especially in old structures in some developing countries. Many structures were reported to fail due to inadequate confinement in concrete columns as large hoop spacing and lack of seismic hoops, as reported after 2008 Sichuan (Wang 2008), 2010 Maule earthquake in Chile (Yen et al. 2011), 2011 Vann earthquake in Turkey (Baran et al. 2012), and 2014 Yunnan earthquake in China (Cheng et al. 2015), etc. Following the spalling of cover concrete at the plastic hinge locations in concrete columns under the effect of earthquake-induced reversed moments, the hooks at the ends of hoops open up because of insufficient anchorage. Once the ends of the hoops open up, the confinement effect on the core concrete diminishes, which in turn causes crushing of concrete in the entire cross section. Large hoop spacing and lack of stirrup anchorage at the plastic hinge locations of columns also lead to buckling of column longitudinal bars. The seismic strengthening of the concrete columns improperly designed or constructed is in an urgent need.

Extensive investigations on the seismic retrofitting of reinforced concrete (RC) columns have been undertaken in recent years. There has been an enormous interest in the research and application of fiber reinforced polymers (FRPs) in RC column seismic retrofitting since the 1980s. The basic concepts and relatively recent survey in the use of FRPs for strengthening of concrete structures are covered in a review article by Triantafillou (2001). Many researchers have proven the effectiveness of applications of conventional FRP materials such as aramid, carbon, and glass in shear and ductility enhancement (Bakis et al. 2002; Benzaid et al. 2008; Teng et al. 2003; Wu et al. 2006). However, due to low fracturing strain capacity of conventional FRPs (around 1.5% for carbon FRP (CFRP), 2% for glass FRP (GFRP) and 3% for aramid FRP (AFRP)), the fiber materials tend to fail sooner due to fiber breakage which causes a loss of confinement and hence the load-carrying capacity as well as the ductility potential. New fiber materials such as polyacetal fiber (PAF), polyethylene naphthalate (PEN) and

polyethylene terephthalate (PET) have properties of large fracturing strain and low stiffness in comparison to aramid, carbon, and glass fibers (Jirawattanasomkul et al. 2013). Previous studies (Anggawidjaja et al. 2006; Dai et al. 2011; Dai et al. 2012) proved that concrete or RC members wrapped by PET and PEN fiber sheets with large fracturing strain could efficiently enhance the ductility of concrete or RC members regardless of their low stiffness. The large fracturing strain allowed the fiber to contribute sufficient shear force at the ultimate state while avoiding fiber rupture.

Corrosion of the reinforcement is one of the major causes of deterioration in reinforced concrete structures. Corrosion damage is usually observed as rust stains and minute cracking over the concrete surface running parallel to the underlying steel bars, as a result of volume increase associated with the formation of corrosion products. Past experiences have shown that reinforcement corrosion reduces the column capacity due to steel area losses. Despite a large body of literature on the influence of reinforcing steel corrosion on the flexural capacity of RC columns with or without FRP strengthening (Li et al. 2014; Pantazopoulou et al. 2001; Ma et al. 2012), there are few works that have dealt with the reduction in shear capacity of RC columns due to the corrosion of stirrups (Xia et al. 2011). Actually, stirrups would be first attacked by chlorides in a chloride environment since they are nearer to the concrete surface than the longitudinal steel bars.

In this paper, an experimental study is presented on the influence of PET warping on shear strength, ductility and energy absorptivity of RC columns with stirrup corrosion before strengthening. The experimental program involved an electrochemical process to accelerate the migration of chlorides from an external electrolyte into the tested columns, a wetting – drying cycle process with a controlled current to speed up the corrosion of the stirrup in the tested columns, the strengthening of corroded columns with PET warping, and a Pseudo static test to determine the shear capacity of the tested beams. The shear performance of PET wrapped RC columns with different corrosion levels in stirrups was examined.

## EXPERIMENTAL PROGRAM

### Details of test setup

A total of 11 RC rectangular columns with footings were constructed, which consisted of four un-strengthened control specimens with different level of stirrup corrosion (designed to be 0, 10%, 15% and 25%) and seven strengthened specimens with different layers of PET fiber warping (1or 2 layers), as indicated in Table 1. The acronym designation adopted for the specimens was as follows: “C” represents corrosion pre-damage, and the number following “C” stands for degree of corrosion of stirrups before strengthening; “L” means PET warping and the last number corresponds to the number of warping layers. For example, specimen “C-10-L-2” is the RC column with expected degree of corrosion of stirrups of 10%, which was warped by 2 layers of PET fiber.

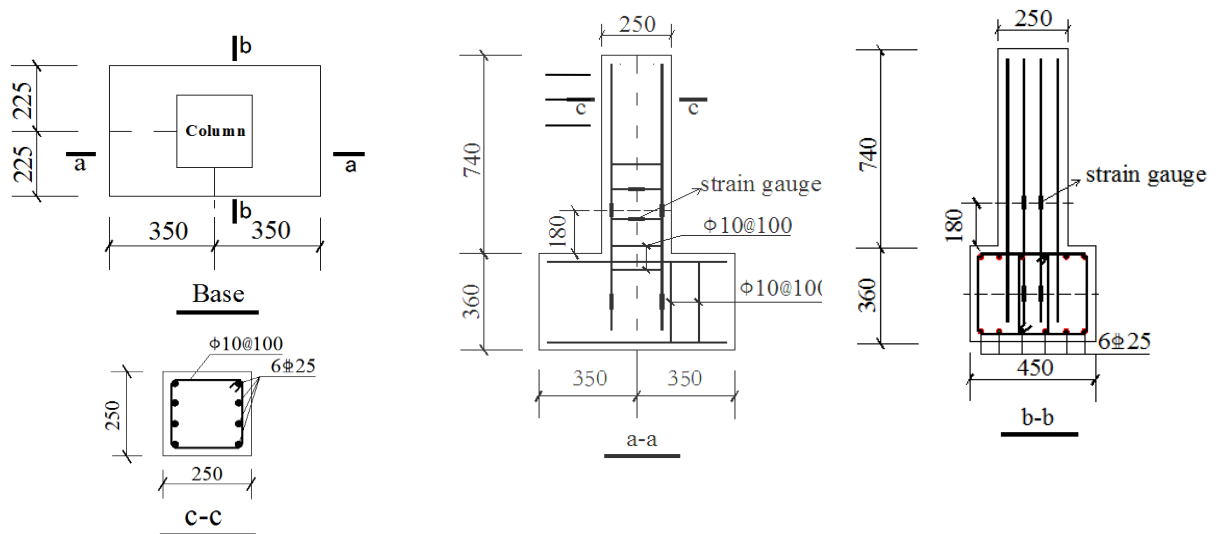


Figure 1 Geometry and reinforcement information of specimens (unit: mm)

The column had a cross section of 250 x 250 mm and a total height of 740 mm. The corners of columns to be strengthened were rounded with a rounding radius of 20mm. The footings had a size of 700 x 450 x 360 mm (length x width x height). Each specimen used eight 25mm deformed bars for longitudinal reinforcement and 10mm plain bars for stirrups spaced at 100mm. The hooks of stirrups had 135-degree bend plus 5db

(db=diameter of stirrup) extension, which is weaker than the minimum requirement of existing seismic design specifications (10 db at 135-degree in JSCE design code (2012), 6 db at 135-degree in ACI 318-11 code (2011), and 5 db at 150-degree in CEB-FIP model code 2010 (2010)), to represent the improper design or construction of stirrups. With the above extension length, the hooks were expected to open up under cyclic loading. The longitudinal reinforcements in the columns were extended into the footing with a sufficient anchorage length. Details of the reinforcement arrangement are shown in Figure 1.

Table 1 Parameters of test specimens

Specimens	Strengthening	Targeted corrosion ratio (%)	PET layers
C-0-L-0	No	0	0
C-0-L-1	Yes	0	1
C-10-L-0	No	10	0
C-10-L-1	Yes	10	1
C-10-L-2	Yes	10	2
C-15-L-0	No	15	0
C-15-L-1	Yes	15	1
C-15-L-2	Yes	15	2
C-25-L-0	No	25	0
C-25-L-1	Yes	25	1
C-25-L-2	Yes	25	2

### Material properties

Same batch of ready mixed concrete were used to cast the specimens. The 28 days cubic (150 x 150 x 150 mm) compressive strength of concrete was 26.6 MPa. Table 2 and 3 show the properties of the reinforcement and PET fiber sheet used in this experiment. The epoxy resin used for PET warping had a tensile strength of 41.0 MPa, elastic modulus of 2.6 GPa and an elongation at break of 1.6%, as provided by the manufacturer.

Table 2 Mechanical properties of steel bars

Bars	Diameter (mm)	Yield stress (MPa)	Ultimate stress (MPa)	Extension ratio (%)	Tensile modulus (MPa)
Longitudinal bar	25	476	580	38.2	$2.12 \times 10^5$
stirrup	10	342	499	36.2	$2.03 \times 10^5$

Table 3 Mechanical properties of PET sheet

Name	Tensile strength $f_{tu}$ (MPa)	Tensile modulus $E_f$ (GPa)	Ultimate strain (%)	Area density $\rho$ (g / m <sup>2</sup> )	Thickness (mm)
PET	719	9.35	$\geq 7\%$	1161	0.841

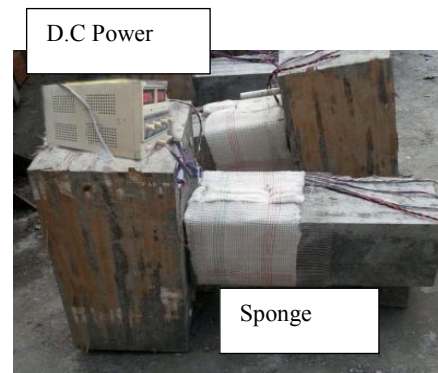
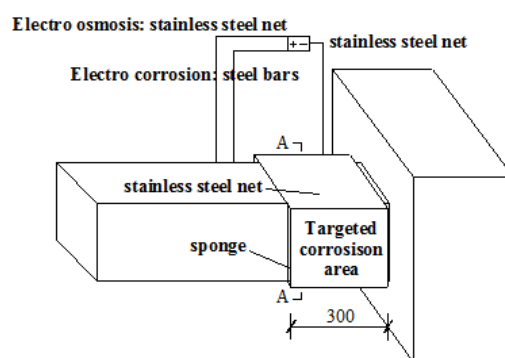


Figure 2 Accelerated corrosion techniques (unit:mm)

### Accelerated corrosion procedure

In order to reduce the experimental time to match the corrosion process and behavior happened in real RC members. An accelerated corrosion procedure suggested by Xia et al. (2011) was applied. As indicated in Figure

2, the accelerate corrosion procedure can be divided into two phases, namely the electro-migration phase and the wetting–drying cycle phase. The specimens were corroded within 300 mm portion of the plastic hinge zone. In the electro-migration phase, chloride ions were electro-migrated into the concrete cover using an electrochemical method. A stainless steel sheet was placed along the longitudinal centroid line of the column. A constant voltage of 30 V was then applied between the outside stainless steel nets and the embedded stainless steel sheets using a DC power source. A wetting–drying cycle process was used immediately after the electro-migration process. Each cycle of the wetting–drying process involved 3 days of drying followed by 4 days of wetting as suggested by Xia et al. (2011) to reach a similar corrosion of steel reinforcement as in a real environment. A current density of 0.20 mA/cm<sup>2</sup> was applied through the stirrup (acting as the anode) and the stainless steel nets (acting as the cathode). Insulation tapes were bonded to longitudinal reinforcement at its intersection with stirrup. The estimated time for corrosion was calculated based on Faraday's law. The wetting–drying cycles lasted for 7, 10 and 16 weeks for the expected degree of corrosion of 10%, 15% and 25%, respectively.

### **Instrumentation and testing procedure**

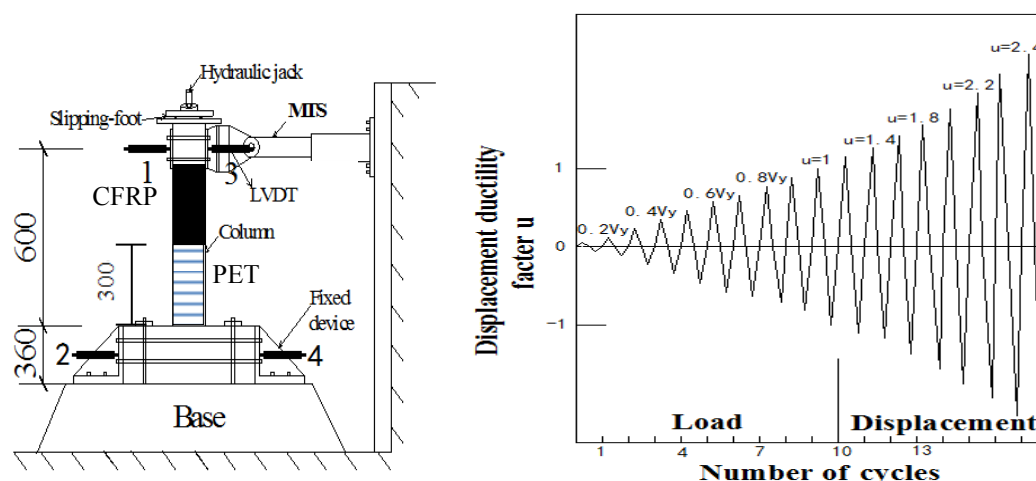


Figure 3 Loading device and loading steps

As shown in Figure 3, the specimens were subjected to a combination of cyclic horizontal load and constant axial load. The compressive vertical load represents the service and dead load of superstructures and equals to 180 kN, which is about 30 % of the expected axial loading capacity of un-corroded control column. A MTS actuator was used to apply the horizontal cyclic load. The cyclic tests were first conducted under load control for load cycles until the yielding of the longitudinal reinforcement, which was approximately evaluated based on the strain gages readings. The horizontal load was adopted to control the loading procedure. In the second phase, the specimens were loaded cyclically under displacement control until the failure of the specimens. The horizontal displacement of the actuator was adopted to control the loading procedure. Load and displacement can be controlled and recorded during the tests by a computer connected to the hydraulic actuator. Load increments and displacement increments between adjacent load cycles are illustrated in Figure 3. Each controlling step lasts for one cycle.

Two transducers (LVDT) were mounted on the rigid frames to measure lateral displacement of columns. Two LVDTs were mounted at the footing to measure horizontal slip and rotation of the footing, as indicated in Figure 3. Strain gages were used to measure the strain development in the flexural reinforcements, shear reinforcements and PET fibers. The location of strain gages is indicated in Figure 1.

## **RESULTS AND DISCUSSIONS**

### **Gravimetric Mass Loss Measurements**

After loading the test specimens to failure, the stirrups were extracted and cleaned for the purpose of calculating mass loss following the ASTM G1-03 Standard (2011). Four coupons with a length of 100 mm within the targeted 300 mm long corrosion area per stirrup per column were used. The weight of the stirrup without corrosion was determined by weighing the 100 mm long stirrup in the uncorroded zone of the same column such that the weight of the extracted coupons after corrosion could be compared to the original weight and the mass loss due to corrosion could be estimated. The average measured mass loss (degree of corrosion) in the stirrup of

the corroded columns is listed in Table 4. It can be concluded that the expected mass losses were achieved in the laboratory.

### Failure mode

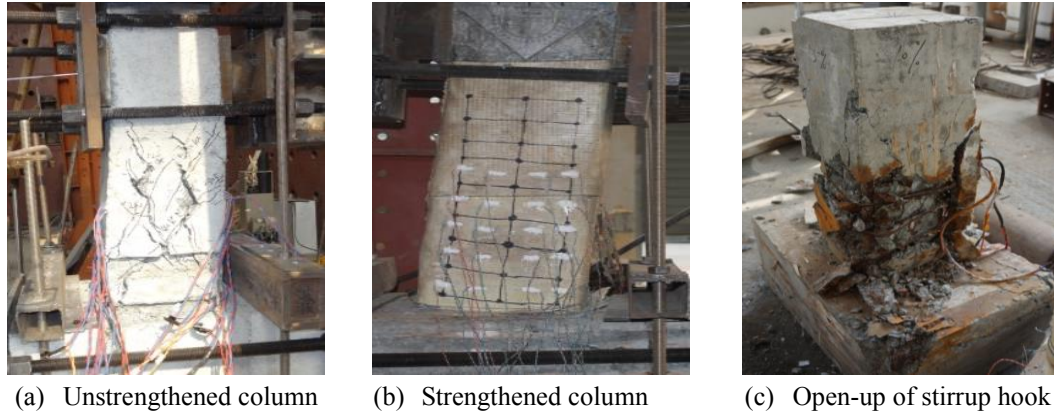


Figure 4 Typical failure modes of test specimens

All un-strengthened specimens showed brittle shear failure with extensive X shape diagonal concrete shear cracks together with the spalling or crushing of cover concrete (Figure 4(a)). After removing the cover concrete, the hooks of stirrups were observed open-up due to insufficient length of hook extension. For all PET strengthened specimens, the PET fiber sheet showed no breakage till the end of the test (Figure 4(b)), while hook open-up of stirrups were also observed after removing the PET sheet and cover concrete (Figure 4(c)). For all the specimens, no buckling of longitudinal reinforcements was observed.

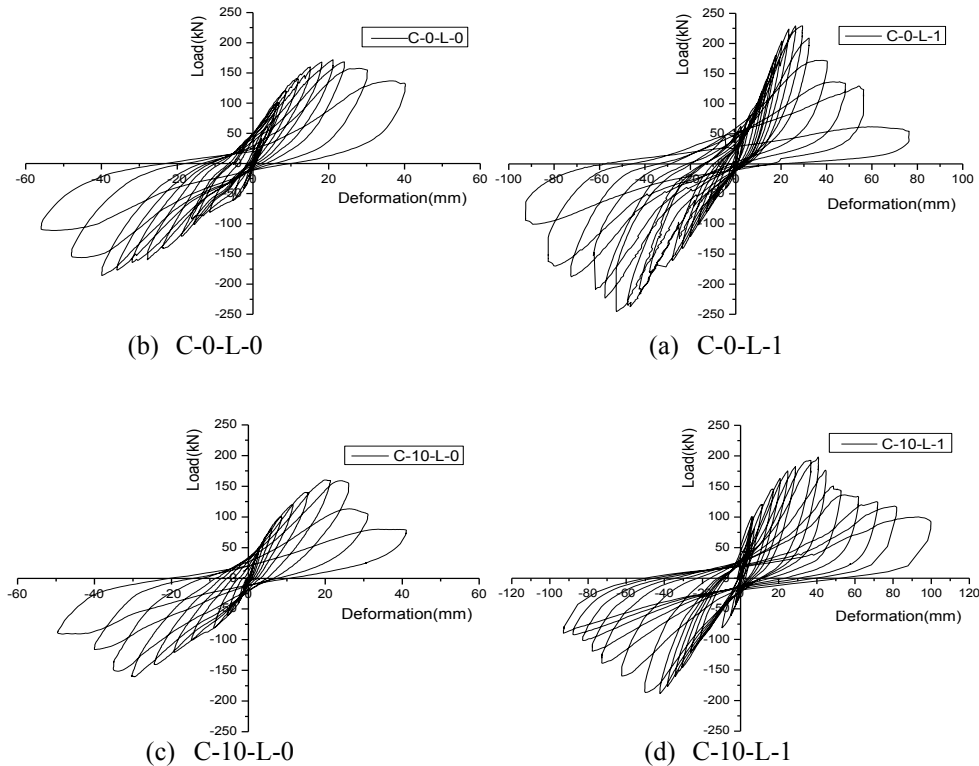


Figure 5 Sample hysteretic responses of the tested specimens

### Hysteretic response and Energy dissipation ratio

Due to space limitation, the sample hysteretic responses of several tested specimens are shown in Figure 5. The skeleton curve of all the specimens are presented in Figure 6. The lateral load at the first yield of longitudinal reinforcement ( $P_y$ ) and the maximum load ( $P_{max}$ ) at the positive and negative bending cycles are summarized in



Table 4. Energy dissipation ratio has been used to evaluate the energy dissipation ability of structures under cyclic loading. The energy dissipation ratio at each load cycle of each specimen can be calculated and the accumulated energy dissipation ( $E_{sum}$ ) is calculated using Eq.1.

$$E_{sum} = \sum_{i=1}^n (E_i) \quad (1)$$

where  $E_i$  is the energy dissipation of  $i$  th load cycle,  $E_{sum}$  is the accumulated energy dissipation,  $n$  is the number of loading cycles. The accumulated energy dissipations of test specimens are presented in Table 4.

### Effect of stirrup corrosion

As shown in Figure 6(e-f) and Table 4, for both unstrengthened and strengthened columns, the yield load, the peak load and accumulated energy dissipation decreased with the increase of degree of stirrup corrosion. The corrosion of the stirrups caused deterioration of the bond between the concrete and the stirrups, and cover concrete cracking, which reduced the effective concrete area for load bearing and energy assumption.

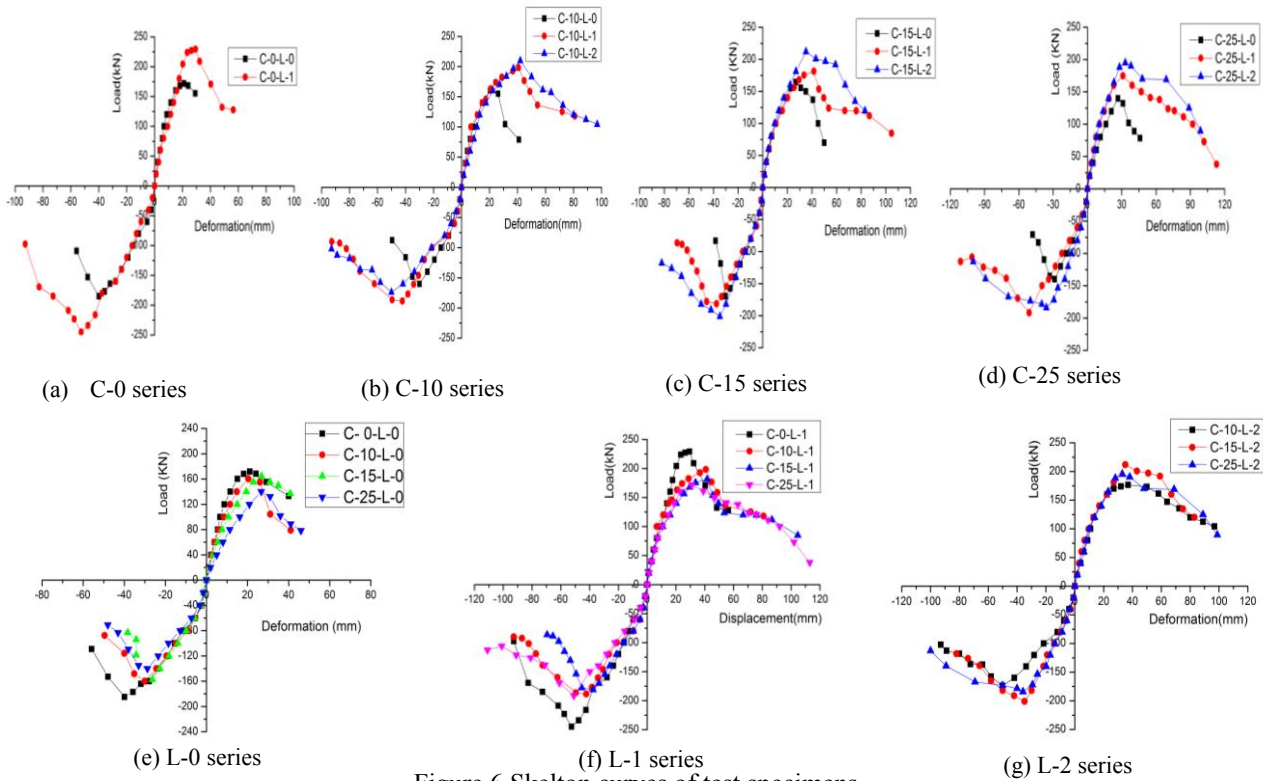


Figure 6 Skelton curves of test specimens

### Effect of PET wrapping

The unstrengthened specimens showed brittle behavior after the peak load, while the specimens with PET wrapping showed sudden drop of load carrying capacity after the peak load to a certain level and then exhibited a ductile response. The peak load was reached after the open-up of hooks of stirrups, which caused the loss of stirrup contributions and spalling of cover concrete. As shown in Figure 6(a-d) and Table 4, the yield load, the peak load and the accumulated energy dissipation after PET wrapping comparing to the unstrengthened columns with similar degree of stirrup corrosion was enhanced. The enhancement was more obvious with the increase of number of PET layers. The effect of stirrup corrosion on the peak load was reduced after the PET wrapping. Although the specimens were designed with insufficient shear capacity, the PET confinement could provide additional shear capacity and confinement to the concrete, which delayed the open-up of stirrups and could still carry the shear force after that.

Table 4 Summary of test results

Specimens	Average corrosion degree	Negative moment		Positive moment		Total energy dissipation
	$\eta_{ave}$	Yield load	Peak load	Yield load	Peak load	$E_{sum}$
	(%)	$P_{y+}$ (kN)	$P_{max+}$ (kN)	$P_{y-}$ (kN)	$P_{max-}$ (kN)	(kN•m)
C-0-L-0	0	151	171.9	-140.7	-185	63.6
C-0-L-1	0	218.7	229.3	-238.8	-245	135.3
C-10-L-0	10.66	140.2	160.3	-130.7	-160	41.9
C-10-L-1	9.91	170.1	198.1	-151.8	-188.5	131.1
C-10-L-2	11.2	175.8	209.7	-146.1	-173.8	148.6
C-15-L-0	15.63	130.8	164.5	-125.2	-169.8	43.9
C-15-L-1	16.26	149.2	181.5	-146.1	-181.3	115.9
C-15-L-2	16.82	174.5	211.9	-189.3	-201	122.4
C-25-L-0	21.66	129.2	140	-95.89	-140	44.1
C-25-L-1	22.78	134.3	175	-169.3	-191.7	162.8
C-25-L-2	19.86	180.5	195.1	-154.2	-184	133.6

## CONCLUSIONS

This paper presented the experimental study on the influence of PET wrapping on shear strength, ductility and energy absorptivity of RC columns with stirrup corrosion before strengthening. The following conclusions can be drawn:

For unstrengthened columns, the yield load, peak load, ductility ratio and energy dissipation ratio decreased with the increase of degree of stirrup corrosion.

The yielding load, peak load and accumulated energy dissipation after PET wrapping comparing to the unstrengthened columns with similar degree of stirrup corrosion was enhanced. The enhancement was more with the increase of number of PET layers.

For uncorroded columns, the ductility ratio was reduced after the PET wrapping, mainly attributing to the sudden drop of load carrying capacity after the open-up of stirrup hooks. For corroded columns, the ductility ratio was slightly increased after the PET wrapping, which indicated that the PET wrapping can compensate the loss of column ductility due to stirrup corrosion.

## ACKNOWLEDGMENTS

The authors gratefully acknowledge the financial support provided by natural science foundation of China (No. 51308494) and the Fundamental Research Funds for the Central Universities of China (No. 513201\*172210251)

## REFERENCES

- ACI 318 Committee. (2011). Building Code Requirements for Structural Concrete (ACI 318-11) and Commentary. In American Concrete Institute (p. 503).
- ASTM G1 –03(2011). Standard practice for preparing, cleaning, and evaluating corrosion test specimens, ASTM International, West Conshohocken, PA.
- Anggawidjaja, D., Ueda, T., Dai, J., & Nakai, H. (2006). Deformation capacity of RC piers wrapped by new fiber-reinforced polymer with large fracture strain. *Cement and Concrete Composites*, 28(10), 914-927.
- Bakis, C., Bank, L. C., Brown, V., Cosenza, E., Davalos, J. F., Lesko, J. J., ... & Triantafillou, T. C. (2002). Fiber-reinforced polymer composites for construction-state-of-the-art review. *Journal of Composites for Construction*, 6(2), 73-87.

- Baran, E., Mertol, H. C., and Gunes, B. (2012). Damage in reinforced-concrete buildings during the 2011 Van, Turkey, earthquakes. *Journal of Performance of Constructed Facilities*, 28(3), 466-479.
- Benzaid, R., Chikh, N. E., & Mesbah, H. (2008). Behaviour of square concrete column confined with GFRP composite wrap. *Journal of civil engineering and management*, 14(2), 115-120.
- CEB-FIP Model Code 2010 (2010). Comité Euro-International du Béton Secrétariat Permanent. Case Postale 88, CH-1015 Lausanne, Switzerland.
- Cheng, J., Wu, Z., Liu, J., Jiang, C., Xu, X., Fang, L., ... & Yang, T. (2015). Preliminary Report on the 3 August 2014, Mw 6.2/Ms 6.5 Ludian, Yunnan-Sichuan Border, Southwest China, Earthquake. *Seismological Research Letters*, 86(3), 750-763.
- Dai, J. G., Bai, Y. L., & Teng, J. G. (2011). Behavior and modeling of concrete confined with FRP composites of large deformability. *Journal of Composites for Construction*.
- Dai, J. G., Lam, L., & Ueda, T. (2012). Seismic retrofit of square RC columns with polyethylene terephthalate (PET) fibre reinforced polymer composites. *Construction and Building Materials*, 27(1), 206-217.
- Gao, Y., Wang, Q., Zhao, B., & Shi, Y. (2014). A rupture blank zone in middle south part of Longmenshan Faults: Effect after Lushan Ms7.0 earthquake of 20 April 2013 in Sichuan, China. *Science China Earth Sciences*, 57(9), 2036-2044.
- Jirawattanasomkul, T., Dai, J. G., Zhang, D., Senda, M., & Ueda, T. (2013). Experimental Study on Shear Behavior of Reinforced-Concrete Members Fully Wrapped with Large Rupture-Strain FRP Composites. *Journal of Composites for Construction*, 18(3), A4013009.
- JSCE. Standard specification for concrete structures (2012): Design. Japan Society of Civil Engineerings.
- Li, J. H., and Li, Y. (2014). "Experimental and Theoretical Study on the Seismic Performance of Corroded RC Circular Columns Strengthened With Hybrid Fiber Reinforced Polymers." *Polym Polym Compos*, 22(8), 653-659.
- Ma, Y., Che, Y., and Gong, J. X. (2012). "Behavior of corrosion damaged circular reinforced concrete columns under cyclic loading." *Constr Build Mater*, 29, 548-556.
- Pantazopoulou, S. J., Bonacci, J. F., Sheikh, S., Thomas, M. D. A., & Hearn, N. (2001). Repair of corrosion-damaged columns with FRP wraps. *Journal of composites for construction*, 5(1), 3-11.
- Tapan, M., and Aboutaha, R. S. (2011). "Effect of steel corrosion and loss of concrete cover on strength of deteriorated RC columns." *Constr Build Mater*, 25(5), 2596-2603.
- Teng, J. G., Chen, J. F., Smith, S. T., & Lam, L. (2003). Behaviour and strength of FRP-strengthened RC structures: a state-of-the-art review. *Proceedings of the ICE-Structures and Buildings*, 156(1), 51-62.
- Triantafillou, T. C. (2001) "Seismic Retrofitting of Structures with Fiber- Reinforced Polymers," *Progress in Structural Engineering and Materials*, 3(1), 57-65. Wang Y., (2008). Lessons learnt from building damages in the Wenchuan earthquake—seismic concept design of buildings [J]. *Journal of Building Structures*, 4, 004.
- Xia, J., Jin, W. L., and Li, L. Y. (2011). Shear performance of reinforced concrete beams with corroded stirrups in chloride environment. *Corrosion Science*, 53(5), 1794-1805.
- Yen, W., Chen, G., Buckle, I., Allen, T., Alzamora, D., Ger, J., and Arias, J. G. (2011). *Post-earthquake reconnaissance report on transportation infrastructure: impact of the February 27, 2010, Offshore Maule Earthquake in Chile* (No. FHWA-HRT-11-030).